Volume 15, Issue 3, 152422 (1-9)

International Journal of Nano Dimension (IJND)

https://dx.doi.org/10.57647/j.ijnd.2024.1503.22

Exploring of structural, electronic, and optical properties of transition metal doped C_{20} clusters

Reza Ghiasi[1,*], Vahid Daneshdoost[2], Rose Tale[2]

[1]*Department of Chemistry, East Tehran Branch, Islamic Azad University, Tehran, Iran.*
[2]*Department of Chemistry, Arak Branch, Islamic Azad University, Arak, Iran.*

[*]**Corresponding author:** rezaghiasi1353@yahoo.com, reza.ghiasi@iau.ac.ir

Original Research

Received:
13 March 2024
Revised:
10 April 2024
Accepted:
14 April 2024
Published online:
15 June 2024

Abstract:

In the current investigation, computational viewpoint of doped C_{20} nano-cage with Zn, Cu^{+}, Ni^{2+}, and Co^{3+} was described at B3LYP*/6-311G(d,p) level of theory in singlet spin state. Vibrational analysis was established retaining of the optimized nano-cage of the minimum potential energy curve. M-C bond lengths, electronic spatial extent (ESE), photoelectron spectrum (PES) and the results of molecular orbital analysis of the studied clusters were reported. QTAIM results were considered to exploration of metal-carbon bonds characters. NICS values were provided to illustration of aromaticity the clusters. Also, doping outcome on the linear and nonlinear optical properties the clusters was demonstrated.

Keywords: C_{20} cluster; Electronic Spatial Extent (ESE); NICS; Photoelectron spectrum (PES); Polarizability

1. Introduction

C_{20} cluster is considered as familiar smallest fullerene is. Preparation and characteristics of this nano-cage have been described [1]. The exploring of the structure and properties of C_{20} cluster has been described in the various researches [2–11]. The prominent construction of C_{20} has been involved the kindnesses of investigators [12, 13].

Nano-clusters play significant role in drug delivery systems [14], then, C_{20} cluster and various anticancer drugs interactions examined. For instance, a computational study of solvent effect on the interaction between the cisplatin and C_{20} informed [15]. In further research, complexation of C_{20} and $M^{+}@C_{20}$ (M^{+} = Li, Na, K) clusters with titanocene dichloride (TDC) reported [16].

Moreover, computational researches of interaction C_{20} cluster with organometallic fragments have been explored structures and properties of these complexes. In a research, quantum mechanics study interaction of C_{20} cage with $Cr(CO)_5$ fragment was reported [17]. In further studies, the interactions of C_{20} cluster with diazene [18] and substituted-diazenes molecules [19] demonstrated.

In the current research, doping effect is explored in the C_{20} clusters with Zn, Cu^{+}, Ni^{2+}, and Co^{3+} cations. Structural parameters, electronic properties, photoelectron spectrum (PES) and aromaticity of the clusters are reported.

2. Computational Methods

Optimizations of the studied molecules were done with the Gaussian 09 package [20]. Our calculations were considered with the B3LYP* method with c3 = 0.15 [21, 22] and the standard 6-311G(d,p) basis set [23–26]. Also, single point calculations were done on the optimized clusters at the PBE1PBE/6-311G(d,p) level of theory. This hybrid functional includes 25% exchange and 75% correlation weighting [27]. The Perdew-Burke-Ernzerhof exchange-correlation functional (PBE) is a very popular non-empirical generalized-gradient approximation (GGA).

Next outcome stationary points, their characteristics as an energy minimum were established using vibrational analysis.

Polarizability and hyperpolarizability values were computed by Multiwfn 3.8 package [28, 29]. The total static first hyperpolarizability (β_{tot}) was calculated from the following formula:

$$\beta_{tot} = \sqrt{\beta_x^2 + \beta_y^2 + \beta_z^2}$$

Where:

$$\beta_i = \beta_{iii} + \frac{1}{3}\sum_{i\neq j}(\beta_{ijj} + \beta_{jij} + \beta_{jji})$$

The Kleinman symmetry show that [30]:

$$\beta_{xyy} = \beta_{yxy} = \beta_{yyx};\ \beta_{yyz} = \beta_{yzy} = \beta_{zyy}, \ldots$$

Hence:

$$\beta_{\text{tot}} = \sqrt{(\beta_{xxx} + \beta_{xyy} + \beta_{xzz})^2 + (\beta_{yyy} + \beta_{yzz} + \beta_{yxx})^2 + (\beta_{zzz}zxx + \beta_{zyy})^2}$$

The results of quantum theory of atoms in molecules (QTAIM) analysis and picturing of the photoelectron spectrum (PES) were given with Multiwfn 3.8 package [28, 29]. The nucleus independent chemical shift (NICS) was provided to elucidate the aromaticity from the magnetic feature. NICS is demarcated as the negative value of the absolute magnetic shielding determined at the ring center [31] or extra suitable point of the structure [32].

3. Results and discussion

3.1 Energetic aspects

C_{20} cluster contains Ih point group. Doped clusters of this cluster with Zn, Cu^+, Ni^{2+}, and Co^{3+} cations reduces its point group to C_{3v}. Optimization of these doped clusters are considered B3LYP*/6-311G(d,p) level of theory in singlet spin state. Figure 1 presents optimized geometries of $[C_{19}Zn]$, $[C_{19}Cu]^+$, $[C_{19}Ni]^{2+}$, and $[C_{19}Co]^{3+}$ clusters. Vibrational analysis of these nano-cages confirms the full-optimized geometries $[C_{19}Zn]$, $[C_{19}Ni]^{2+}$, and $[C_{19}Co]^{3+}$ reveal any imaginary frequencies, illustrative that they are placed on actual minima in the potential surface.
C_{3v} geometry of $[C_{19}Cu]^+$ cage specifies an imaginary frequency at -309.00 cm^{-1}. So, this geometry is a transition state. Performance additional calculation changes this geometry to the most stable isomer. This geometry is more stable than C_{3v}-ismoer (2.01 kcal/mol). This states the prominence of the geometrical fit for manipulative stable

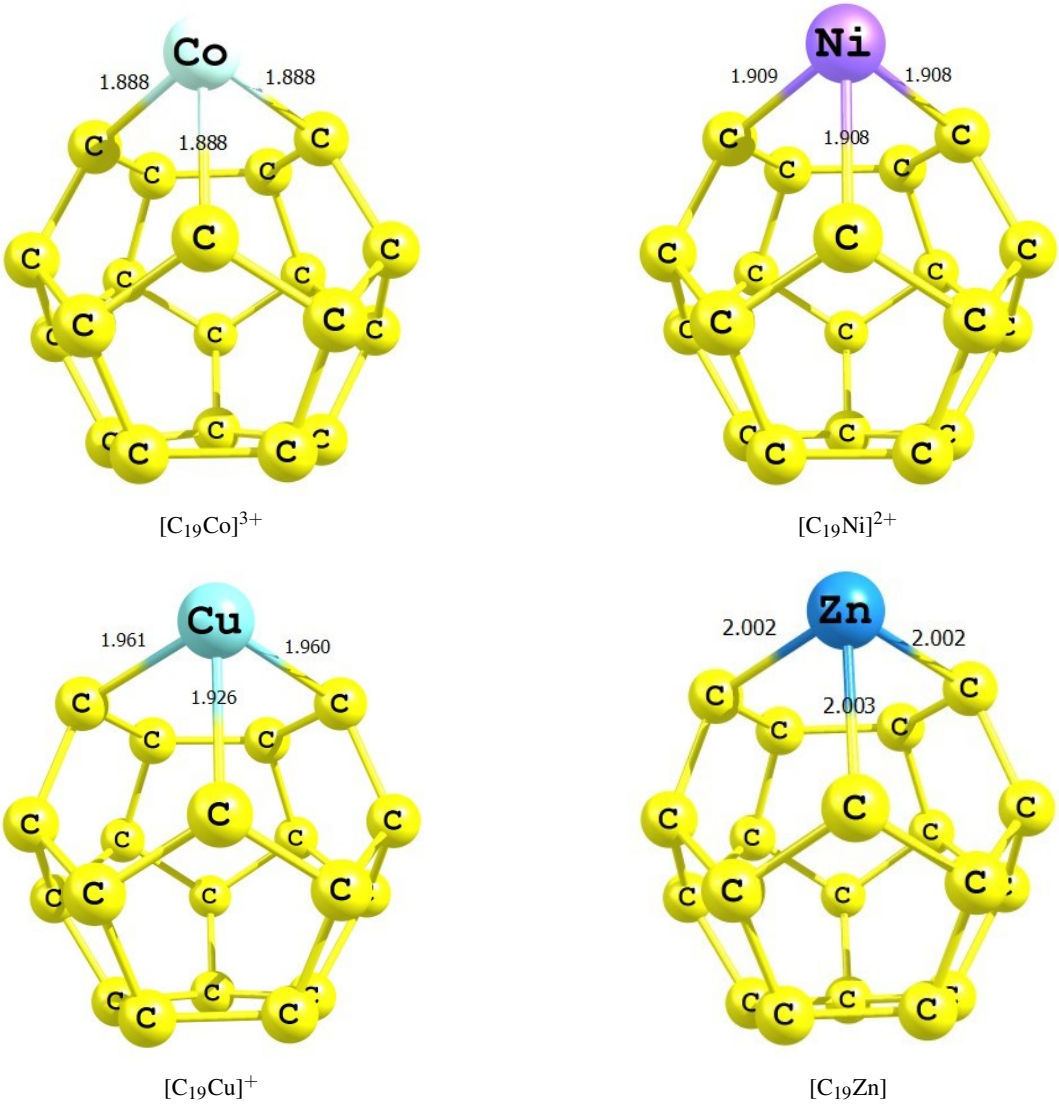

$[C_{19}Co]^{3+}$ $[C_{19}Ni]^{2+}$

$[C_{19}Cu]^+$ $[C_{19}Zn]$

Figure 1. Optimized geometries and M-C bond lengths of $[C_{19}Co]^{3+}$, $[C_{19}Ni]^{2+}$, $[C_{19}Cu]^+$, $[C_{19}Zn]$ molecules at B3LYP*/6-311g(d,p) level of theory in singlet state.

clusters.

3.2 Ionization potential and electron affinity

Vertical electron affinity (EA_v) and vertical ionization potential (IP_v) of the studied clusters are provided (Table 1). It can be deduced, EA_v and IP_v values decrease as: Co > Ni > Cu > Zn. Consequently, these parameters enhance with decreasing of metal atomic number (Z_M). It is clearly to appreciate that the smaller EA_v values than those of the IP_v, identifying that these clusters can positively accept electrons. Thus, these clusters can performance as the electrophilic reagents in the chemical reactions.

3.3 Polarity

Calculated dipole moments of the studied clusters are gathered in Table 1. These values display that $[C_{19}Co]^{3+}$ cluster is non-polar, although other clusters are polar. $[C_{19}Zn]$ cluster tells most polarity between considered clusters.

3.4 Electronic spatial extent (ESE)

ESE is a physical property taking a single number (in atomic unit) defines the size of the molecule. ESE is calculated as the anticipation value of the electron density times the distance from the center of mass of a molecule. More, it is characteristics physical property of the electron density volume around the molecule. As the extent value enhances as electron cloud becomes more defused. In this case, computed ESE value of C_{20} cluster is 2074.95 a.u., however larger values have been found in the doped clusters (Table 1).

3.5 Bond distances

Metal-carbon bond distances of the studied clusters are presented in Figure 1. It can be detected M-C bond distances decrease as: Zn > Cu > Ni > Co. These bond lengths are similar M-C bond distances in the alkyl-transition metal complexes [33–36]. Equal M-C bonds are found in the presence of Zn, Ni^{2+}, and Co^{3+}. Nonetheless, in the presence of Cu^{+} cation one of the Cu-C bond is shorter than two other bonds. These bond lengths variations are attributed to Jahn-Teller distortion in this cluster.

3.6 QTAIM

The outcomes of QTAIM analyses are valuable to exploring of metal-carbon bonds in the investigated clusters. Computed electron density at three bond critical point of metal-carbon bonds (ρ BCP) are 0.1375 (M=Co^{3+}), 0.1267 (M=Ni^{2+}), and 0.0943 (M=Zn) e.$Å^{-3}$. Computed ρ BCP values of two Cu-C bonds are 0.1046 e.$Å^{-3}$ and other bond is 0.11589 e.$Å^{-3}$. It can be deduced, average of ρ BCP values for three bonds reduce with enhancing of Z_M. Thus, the trend of M-C bond strength alterations as: Zn < Cu < Ni < Co.

Computed Laplacian of electron density at three bond critical point of metal-carbon bonds ($\nabla^2\rho$BCP) are 0.1826 (M=Co^{3+}), 0.1111 (Ni^{2+}), and 0.2232 (Zn) e.$Å^{-5}$. Computed $\nabla^2\rho$BCP values of two Cu-C bonds are 0.2105 e.$Å^{-5}$ and other bond is 0.1448 e.$Å^{-5}$.

Computed density energy (HBCP) at three bond critical point of metal-carbon bonds are −0.0559 (Co^{3+}), −0.0520 (Ni^{2+}), and −0.0332 (Zn) e2.$Å^{-4}$. Computed HBCP values of two Cu-C bonds are −0.0389 e^2.$Å^{-4}$and other bond is −0.0465 e^2.$Å^{-4}$.

Computed potential density energy (V_{BCP}) at three bond critical point of metal-carbon bonds are −0.1574 (M=Co^{3+}), −0.1318 (M=Ni^{2+}), and −0.1221 (M=Zn) e^2.$Å^{-4}$. Compute V_{BCP} values of two Cu-C bonds are −0.1299 e^2.$Å^{-4}$ and other bond is −0.1293 e^2.$Å^{-4}$.

Positive $\nabla^2\rho$BCP and negative HBCP at BCP(M-C) bonds tell that the metal-carbon bonds be classified to intermediate bonds between covalent and ionic bonds. Similar arrangement is found in organometallic compounds.

3.7 Molecular orbital analysis

Figure 2 exhibits plots of frontier orbitals of the studied clusters. Results of this analysis are shown in Table 2. It can be observed; larger E(HOMO) and E(LUMO) with enhancing of Z_M. Thus, stability of HOMO and LUMO reduce with enhancing of Z_M. On the other hand, computed HOMO-LUMO gap values variate as Zn > Cu > Ni > Co. Accordingly, $C_{19}Zn$ cluster reveal the most electrical conductivity. Calculated chemical potential values rise with enhancing of atomic metal number. Electrophilicity values of the clusters enhance as Co < Ni < Cu < Zn. Then, the functional influences on the frontier orbital energy and HOMO-LUMO gap values are provided. Results

Table 1. Vertical ionization potential (IP_v, eV), vertical electron affinity (EA_v, eV), dipole moment (μ, Debye) electronic spatial extent (ESE, a.u.), NICS (ppm) values of $[C_{19}Co]^{3+}$, $[C_{19}Ni]^{2+}$, $[C_{19}Cu]^{+}$, $[C_{19}Zn]$ molecules at B3LYP*/6-311G(d,p) level of theory.

Cluster	IP_v	EA_v	μ	ESE	NICS
C_{20}	6.83	1.49	0.00	2074.95	−19.77
$C_{19}Co^{3+}$	22.28	16.43	0.05	2533.15	−33.52
$C_{19}Ni^{2+}$	16.49	11.48	2.34	2590.83	−34.44
$C_{19}Cu^{+}$	12.06	6.92	1.52	2668.79	−34.46
$C_{19}Zn$	7.45	1.29	3.10	2752.30	−45.99

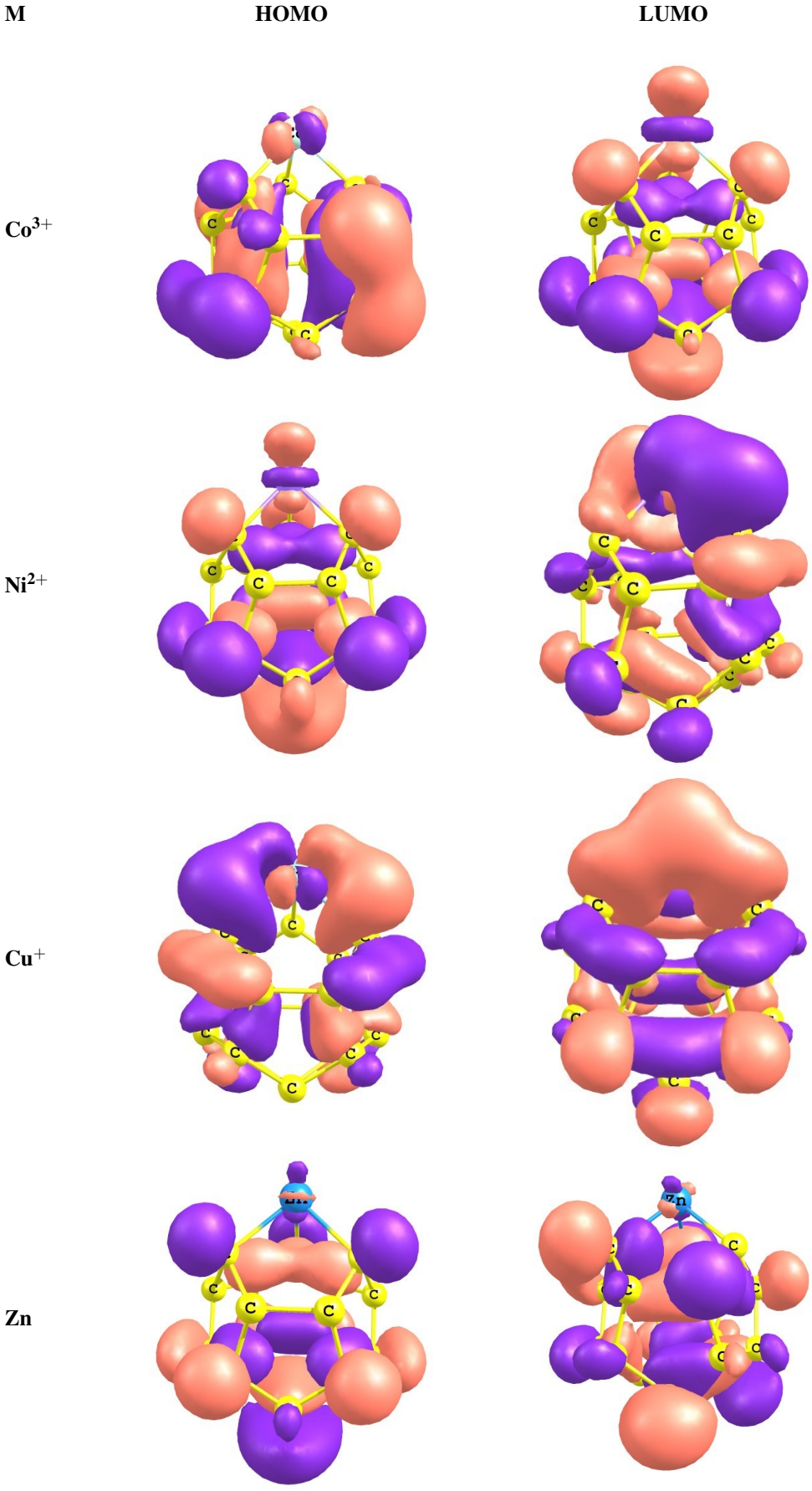

Figure 2. Plots of frontier orbitals of the $[C_{19}Co]^{3+}$, $[C_{19}Ni]^{2+}$, $[C_{19}Cu]^{+}$, $[C_{19}Zn]$ molecules.

of calculations of single point on the optimized clusters at the PBE1PBE/6-311G(d,p) level of theory are listed in Table 2. It can be found, identical variations of E(HOMO), E(LUMO) and gap values at two level of theory.

3.8 Photoelectron spectroscopy

Theoretical photoelectron spectra (PES) of the investigated clusters are shown in Figure 3. These spectra are constructed on generalized Koopmans' theorem. It can be inferred that the initial peaks are seemed at 5.71, 12.06, 16.49, and 22.28, eV in the $[C_{19}Zn]$, $[C_{19}Cu]^{+}$, $[C_{19}Ni]^{3+}$ and $[C_{19}Co]^{3+}$ clusters, respectively. It basically inferred first ionization potential values enhance as: Zn < Cu < Ni < Co.

3.9 Aromaticity

NICS data are valuable information about aromaticity in the various systems [37–50]. NICS values of C_{20} and $[C_{19}M]^{n}$ clusters are computed to illustration of aromaticity in these systems (Table 1). Negative NICS values reveal aromaticity character of these clusters. It can be immediately know larger aromaticity in $[C_{19}M]^{n}$ clusters than C_{20} cluster. Aromaticity of clusters has been increased with enhancing of Z_M. Therefore, aromaticity of clusters increases with increasing of Z_M.

3.10 Polarizability

α_{iso} data (static isotropic polarizability) of the C_{20} and $[C_{19}M]^{n}$ clusters are included in Table 3. It immediately

Table 2. Frontier orbital energy, HOMO-LUMO gap, chemical potential (μ) and electrophilicty (ω) values (in eV) $[C_{19}Co]^{3+}$, $[C_{19}Ni]^{2+}$, $[C_{19}Cu]^{+}$, $[C_{19}Zn]$ molecules at (a)B3LYP*/6-311G(d,p) (b) B3LYP*/6-311G(d,p)//PBE1PBE/6311G(d,p) level of theory.

	level a					Level b		
Cluster	**E(HOMO)**	**E(LUMO)**	**Gap**	μ	ω	**E(HOMO)**	**E(LUMO)**	**Gap**
$\mathbf{C_{19}Co^{3+}}$	−20.28	−18.31	1.98	−19.30	188.32	−21.00	−18.53	2.47
$\mathbf{C_{19}Ni^{2+}}$	−14.67	−13.26	1.41	−13.97	138.03	−15.43	−13.42	2.01
$\mathbf{C_{19}Cu^{+}}$	−10.11	−8.73	1.39	−9.42	64.04	−10.98	−8.93	2.06
$\mathbf{C_{19}Zn}$	−5.71	−3.07	2.64	−4.39	7.30	−6.43	−3.20	3.22

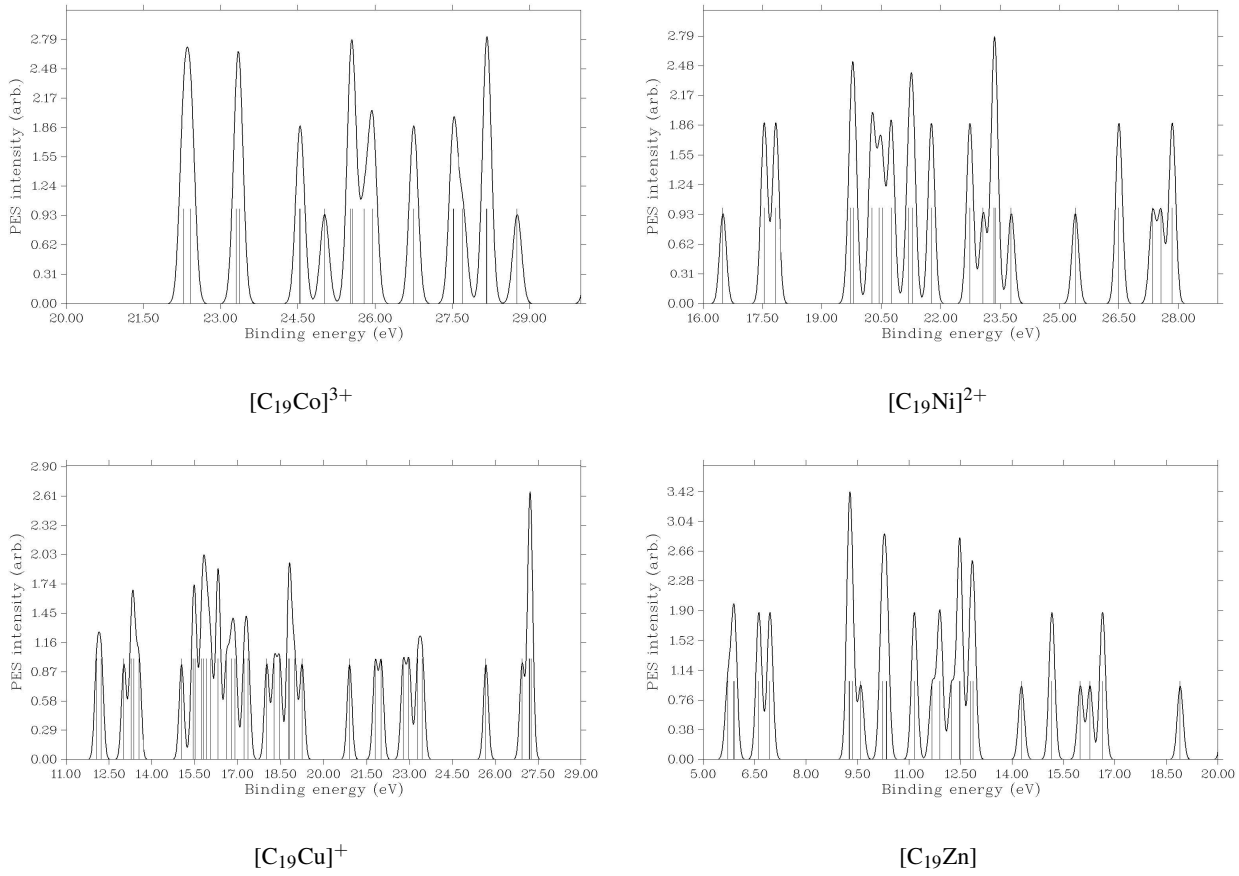

$[C_{19}Co]^{3+}$ $[C_{19}Ni]^{2+}$

$[C_{19}Cu]^{+}$ $[C_{19}Zn]$

Figure 3. Photoelectron spectra of $[C_{19}Co]^{3+}$, $[C_{19}Ni]^{2+}$, $[C_{19}Cu]^{+}$, $[C_{19}Zn]$ clusters.

Table 3. Static isotropic polarizabilities values (α_{iso}, a.u.), static first hyperpolarizability values (β_{tot}, a.u.), dynamic polarizability ($\alpha(-\omega;\omega)$, a.u.), dynamic first hyperpolarizability values ($\beta(-2\omega;\omega,\omega)$, a.u.), scattering hyperpolarizability (β_{HRS} in a.u.) of $[C_{19}Co]^{3+}$, $[C_{19}Ni]^{2+}$, $[C_{19}Cu]^{+}$, $[C_{19}Zn]$ molecules at w = 0.065600 (694.56 nm) at B3LYP*/6-311G(d,p) level of theory.

Cluster	α_{iso}	β_{tot}	$\alpha(-\omega;\omega)$	$\beta(-2\omega;\omega,\omega)$
$\mathbf{C_{19}Co^{3+}}$	164.81	89.03	171.35	1806.29
$\mathbf{C_{19}Ni^{2+}}$	172.01	575.32	186.83	774.44
$\mathbf{C_{19}Cu^{+}}$	179.69	449.43	201.93	2322.73
$\mathbf{C_{19}Zn}$	186.85	1121.60	204.75	833.03

knows larger α_{iso} values with enhancing of Z_M. These computed parameters make evident linear optical properties of clusters, and the attendance of polarizabilities is owed to asymmetric electronic density distribution in these clusters. Dynamic polarizabilities are given from frequency-dependent polarizability. In this work, the incident-frequency (ω) effect on the first polarizability is considered at applied frequencies of 694.56 nm. Direct current second harmonic generation (DCSHG) is employed to calculation of the frequency-dependent polarizability $\alpha(\omega)$. Compute polarizability data ($\alpha_{iso}(-\omega;\omega)$) corresponding to 694.56 nm incident light for the investigated clusters are listed in Table 3. It can be observed, $\alpha_{iso}(-\omega;\omega)$ values decrease as: Zn > Cu > Ni > Co. The similar trend finds in the isotropic polarizability variations.

3.11 Hyperpolarizability

β_{tot} values (static first hyperpolarizability) of the investigated clusters are evaluated (Table 3). $C_{19}Zn$ cluster reveals largest β_{tot} value. It must be noticed that electronic properties notably influence to hyperpolarizability response, and the more variants in dipole moment give the higher hyperpolarizabilities parameters.

The incident-frequency (ω) effect is revealed on the β_{tot} data at applied frequencies of 694.56 nm. $\beta(\omega)$ values (frequency-dependent first hyperpolarizability) are computed with DCSHG.

Frequency-dependent first hyperpolarizability would advise supportive data for judging dynamic first hyperpolarizability. The first hyperpolarizability data ($\beta(-2\omega;\omega,\omega)$) corresponding to w = 0.065600 (694.56 nm) incident light are estimated for the investigated clusters (Table 3). $C_{19}Cu^{+}$ cluster indicates largest $\beta(-2\omega;\omega,\omega)$ value.

4. Conclusion

Doping of C_{20} cluster with Zn, Cu^{+}, Ni^{2+}, and Co^{3+} cations at B3LYP*/6-311g(d,p) level of theory in illustrated C_{3v} point group for optimized structure of $[C_{19}Zn]$, $[C_{19}Ni]^{2+}$ and $[C_{19}Co]^{3+}$ clusters. In contrast, $[C_{19}Cu]^{+}$ cluster distorted from C_{3v} symmetry. Equal metal carbon bond lengths were found for Zn, Ni and Co. but, two of the Cu-C was longer than other bond in $[C_{19}Cu]^{+}$ cluster. Aromaticity of clusters reduced with decreasing of Z_M. Computed α_{iso} and $\alpha_{iso}(-\omega;\omega)$ values enhanced with increasing of Z_M. $[C_{19}Zn]$ and $[C_{19}Cu]^{+}$ clusters revealed largest β_{tot} and $\beta(-2\omega;\omega,\omega)$ values, respectively.

Authors Contributions
All authors have contributed equally to prepare the paper.

Availability of Data and Materials
The data that support the findings of this study are available from the corresponding author upon reasonable request.

Conflict of Interests
The authors declare that they have no known competing financial interests or personal relationships that could have appeared to influence the work reported in this paper.

References

[1] H. Prinzbach, A. Weiler, P. Landenberger, F. Wahl, J. Worth, L.T. Scott, M.D. Gelmont, D. Olevano, and B.V. Issendorff. "Gas-phase production and photoelectron spectroscopy of the smallest fullerene, C_{20}.". *Nature*, **407**:60–63, 2000. DOI: https://doi.org/10.1038/35024037.

[2] E.J. Bylaska, P.R. Taylor, R. Kawai, and J.H. Weare. "LDA Predictions of C_{20} Isomerizations: Neutral and Charged Species.". *J. Phys. Chem. A*, **100**:6966–6972, 1996. DOI: https://doi.org/10.1021/jp9528323.

[3] J.C. Grossman, L. Mitas, and K. Raghavachari. "Structure and Stability of Molecular Carbon: Importance of Electron Correlation.". *Phys. Rev. Lett.*, **750**:3870–3873, 1995. DOI: https://doi.org/10.1103/PhysRevLett.75.3870.

[4] J.M. .L.Martin, J. El-Yazal, and J. Francois. "On the structure and vibrational frequencies of C20. Chem.". *Phys. Lett.*, **248**:345–352, 1996. DOI: https://doi.org/10.1016/0009-2614(95)01334-2.

[5] S. Sokolova, A. Luchow, and J.B. Anderson. "Energetics of carbon clusters C_{20} from all-electron quantum Monte Carlo calculations.". *Chem. Phys. Lett.*, **323**: 229–233, 2000. DOI: https://doi.org/10.1016/S0009-2614(00)00554-6.

[6] R. Taylor, E. Bylaska, J.H. Weare, and R. Kawai. "C20: fullerene, bowl or ring? New results from coupled-cluster calculations.". *Chem. Phys. Lett.*, **235**: 558–563, 1995. DOI: https://doi.org/10.1016/0009-2614(95)00161-V.

[7] Z. Wang, P. Day, and R. Pachte. "Ab initio study of C_{20} isomers: geometry and vibrational frequencies.". *Chem.Phys. Lett.*, **248**:121–126, 1996. DOI: https://doi.org/10.1016/0009-2614(95)01299-0.

[8] C. Zhanga, W. Sun, and Z. Caob. "Most stable structure of fullerene[20] and its novel activity toward addition of alkene: A theoretical study.". *J. Chem. Physics*, **126**:144306, 2007. DOI: https://doi.org/10.1063/1.2716642.

[9] M.Z. Kassaee, F. Buazar, and M. Koohi. "Heteroatom impacts on structure, stability and aromaticity of X_nC_{20-n} fullerenes: A theoretical prediction.". *Journal of Molecular Structure: THEOCHEM*, **940**:19–28, 2010. DOI: https://doi.org/10.1016/j.theochem.2009.10.002.

[10] R. Ghiasi and M.Z. Fashami. "Tautomeric transformations and reactivity of isoindole and sila-indole: A computational study.". *Journal of Theoretical and Computational Chemistry*, **13**:1450041–1–14, 2014. DOI: https://doi.org/10.1142/S0219633614500412.

[11] H. Alavi and R. Ghiasi. "A theoretical study of solvent effect on the interaction of C_{20} and N_2H_2". *J. Struc. Chem.*, **58**:30–37, 2017. DOI: https://doi.org/10.1134/S002247661701005X.

[12] Z. Chen, T. Heine, H. Jiao, A. Hirsch, W. Thiel, and P.v.R. Schleyer. "Theoretical Studies on the Smallest Fullerene: from Monomer to Oligomers and Solid States.". *Chem. Eur. J.*, **10**:963–970, 2004. DOI: https://doi.org/10.1002/chem.200305538.

[13] J. Luo, L.M. Peng, Z.Q. Xue, and J.L. Wu. "Positive electron affinity of fullerenes: Its effect and origin.". *J. Chem. Phys.*, **120**:7998–8001, 2004. DOI: https://doi.org/10.1063/1.1691397.

[14] H. Ghanbari, B.G. Cousins, and A.M. Seifalian. "A nanocage for nanomedicine: Polyhedral oligomeric silsesquioxane (POSS).". *Macromol Rapid Commun.*, **32**:1032–1046, 2011.

[15] Z. Kazemi, R. Ghiasi, and S. Jamehbozorgi. "Analysis of the Interaction Between the C_{20} Cage and cis-$PtCl_2(NH_3)_2$: A DFT Investigation of the Solvent Effect, Structures, Properties, and Topologies.". *Journal of Structural Chemistry*, **59**:1044–1051, 2018. DOI: https://doi.org/10.1134/S0022476618050050.

[16] R. Ghiasi, M. Rahimi, and R. Ahmadi. "Quantum-chemical investigation into the complexation of titanocene dichloride with C_{20} and $M^+@C_{20}$ (M^+ = Li, Na, K) cages.". *Journal of Structural Chemistry*, **61**:1681–1690, 2020. DOI: https://doi.org/10.1134/S0022476620110025.

[17] R. Ghiasi and N. Sadeghi. "Evolution of the interaction between C_{20} cage and $Cr(CO)_5$: A solvent effect, QTAIM and EDA investigation.". *Journal of Theoretical and Computational Chemistry*, **16**:1750007, 2017. DOI: https://doi.org/10.1142/S0219633617500079.

[18] H. Alavi and R. Ghiasi. "A theoretical study of the solvent effect on the interaction of C_{20} and N_2H_2.". *Journal of Structural Chemistry*, **58**:30–37, 2017. DOI: https://doi.org/10.1134/S002247661701005X.

[19] R. Ghiasi, M.Z. Fashami, and A.H. Hakimioun. "A density functional approach toward structural features and properties of $C_{20}\ldots N_2X_2$ (X = H, F, Cl, Br, Me) molecules.". *Journal of Theoretical and Computational Chemistry*, **13**:1450023, 2014. DOI: https://doi.org/10.1142/S0219633614500230.

[20] M.J. Frisch, G.W. Trucks, H.B. Schlegel, G.E. Scuseria, M.A. Robb, et al. *Gaussian 09, Revision A.02*. Gaussian, Inc.: Wallingford, CT, 2009.

[21] R.G. Parr and W. Yang. *"Density-Function Theory of Atoms and Molecules."*. Oxford University Press: Oxford, UK, 1989.

[22] O. Salomon, M. Reiher, and B. A.Hess. "Assertion and validation of the performance of the B3LYP* functional for the first transition metal row and the G2 test set.". *J. Chem. Phys.*, **117**:4729–4737, 2002. DOI: https://doi.org/10.1063/1.1493179.

[23] P.J. Hay. "basis sets for molecular calculations-representation of 3D orbitals in transition-metal atoms.". *J. Chem. Phys.*, **66**:4377–4384, 1977. DOI: https://doi.org/10.1063/1.433731.

[24] R. Krishnan, J.S. Binkley, R. Seeger, and J.A. Pople. "self consistent molecular orbital methods. XX. A basis set for correlated wave functions.". *J. Chem. Phys.*, **72**:650–654, 1980. DOI: https://doi.org/10.1063/1.438955.

[25] A.D. McLean and G.S. Chandler. "Contracted Gaussian-basis sets for molecular calculations. 1. 2nd row atoms, Z=11-18.". *J. Chem. Phys.*, **72**:5639–5648, 1980. DOI: https://doi.org/10.1063/1.438980.

[26] A.J.H. Wachters. "Gaussian basis set for molecular wavefunctions containing third-row atoms.". *J. Chem. Phys.*, **52**:1033–1036, 1970. DOI: https://doi.org/10.1063/1.1673095.

[27] C. Adamo and V. Barone. "Toward reliable density functional methods without adjustable parameters: The PBE0 model.". *J. Chem. Phys.*, **110**:6158–6169, 1999. DOI: https://doi.org/10.1063/1.478522.

[28] T. Lu and F. Chen. "Quantitative molecular surface analysis module:.". *J. Mol. Graph. Model.*, **38**:314–323, 2012. DOI: https://doi.org/10.1016/j.jmgm.2012.07.004.

[29] T. Lu and F. Chen. "Multiwfn: A Multifunctional Wavefunction Analyzer.". *J. Comp. Chem.*, **33**:580–592, 2012. DOI: https://doi.org/10.1002/jcc.22885.

[30] D.A. Keleiman. "Nonlinear Dielectric Polarization in Optical Media.". *Phy. Rev.*, **126**:1977–1979, 1962. DOI: https://doi.org/10.1103/PhysRev.126.1977.

[31] P.v.R.Schleyer, C. Maerker, A. Dransfeld, H.Jiao, and N.J.R.v.E. Hommes. "Nucleus-Independent Chemical Shifts: A Simple and Efficient Aromaticity Probe.". *J. Am. Chem. Soc.*, **118**:6317– 6318, 1996. DOI: https://doi.org/10.1021/ja960582d.

[32] M.K. Cyranski, T.M. Krygowski, M. Wisiorowski, N.J.R. Hommes, and P.v.R. Schleyer. *Angew. Chem., Int. Ed.*, **37**:177–180, 1988.

[33] A.H. Mousa, A.V. Polukeev, J. Hansson, and O.F. Wendt. "Carboxylation of the Ni-Me Bond in an Electron-Rich Unsymmetrical PCN Pincer Nickel Complex.". *Organometallics*, **39**:1553–1560, 2020. DOI: https://doi.org/10.1021/acs.organomet.9b00817.

[34] M. Perez-Jimenez, J. Campos, J. Jover, S. Alvarez, and E. Carmona. "Coordination of E–C Bonds (E = Zn, Mg, Al) and the Zn-H Bonds of (C_5Me_5)ZnH and (C_5Me_5)ZnZnH across a Quadruply Bonded Dimolybdenum Dihydride Complex.". *Organometallics*, **41**:3225–3236, 2022. DOI: https://doi.org/10.1021/acs.organomet.2c00216.

[35] S.T. Shreiber, P.T. Kaplan, R.P. Hughes, M. Vasiliu, D.A. Dixon, R.E. Cramer, and D.A. Vicic. "Syntheses, solution behavior, and computational bond length analyses of trifluoromethyl and perfluoroethyl cuprate salts.". *Journal of Fluorine Chemistry*, **234**:109518, 2020. DOI: https://doi.org/10.1016/j.jfluchem.2020.109518.

[36] T. Spataru and R.L. Birke. "Carbon-Cobalt Bond Distance and Bond Cleavage in One-Electron Reduced Methylcobalamin: A Failure of the Conventional DFT Method.". *J. Phys. Chem. A*, **110**:8599–8604, 2006. DOI: https://doi.org/10.1021/jp062741d.

[37] R. Ghiasi. "A computational study of the arsabenzenes: Structure, properties and aromaticity.". *Journal of Organometallic Chemistry*, **690**:4761–4767, 2005. DOI: https://doi.org/10.1016/j.jorganchem.2005.07.069.

[38] R. Ghiasi. "The mono- and di-silanaphthalene: Structure, properties, and aromaticity.". *Journal of Molecular Structure: THEOCHEM*, **718**:225–233, 2005. DOI: https://doi.org/10.1016/j.theochem.2004.11.038.

[39] R. Ghiasi. "Theoretical study of the properties of fluoroborthiin and fluoroboroxine.". *Journal of Molecular Structure: THEOCHEM*, **853**:77–81, 2008. DOI: https://doi.org/10.1016/j.theochem.2007.12.007.

[40] R. Ghiasi. "Theoretical study of classical isomers tropylium, azatropylium, phosphatropylium, and arsatropylium cations: Structure, properties and aromaticity.". *Main Group Chemistry*, **7**:147–154, 2008. DOI: https://doi.org/10.1080/10241220802436271.

[41] R. Ghiasi and M. Monajjemi. "Theoretical study of borthiin and its derivatives: Structure and aromaticity.". *Journal of Sulfur Chemistry*, **28**:505–511, 2007. DOI: https://doi.org/10.1080/17415990701516440.

[42] R. Ghiasi and M. Monajjemi. "Theoretical study of interaction of alkaline earth metal with $C_4O_4^{2-}$ and $C_4S_4^{2-}$: Structure, electronic properties and aromaticity.". *Journal of Sulfur Chemistry*, **28**:537–546, 2007. DOI: https://doi.org/10.1080/17415990701561263.

[43] R. Ghiasi. "Theoretical study of Borazanaphthalene and its mono-Fluorinated derivatives: Structure and properties.". *Main Group Chemistry*, **6**:43–51, 2007. DOI: https://doi.org/10.1080/10241220701697858.

[44] R. Ghiasi and M. Monnajemi. "Theoretical studies on the structure and aromaticity of 1H-indene and mono-sila-1H-indene.". *Journal of the Korean Chemical Society*, **50**:281–290, 2006. DOI: https://doi.org/10.5012/jkcs.2006.50.4.281.

[45] R. Ghiasi. "Theoretical studies on the structures, properties, and aromaticity of germatropylium cations.". *Main Group Chemistry*, **5**:203–214, 2006. DOI: https://doi.org/10.1080/10241220701458384.

[46] R. Ghiasi. "Arsacyclopentadienyl anions: Structure, properties and aromaticity.". *Main Group Chemistry*, **5**:153–161, 2006. DOI: https://doi.org/10.1080/10241220701414759.

[47] R. Ghiasi, M. Monajjemi, E.E. Mokarram, and P. Makkipour. "Theoretical studies on the structures, properties, and aromaticities of fluorinated arsabenzenes.". *Journal of Structural Chemistry*, **49**:600–605,

2008. DOI: https://doi.org/10.1007/s10947-008-0083-7.

[48] H. Pasdar and R. Ghiasi. "Effect of substitution on the structures, properties, and aromaticity of 1-H-boratabenzene anion.". *Main Group Chemistry*, **8**:143–150, 2009. DOI: https://doi.org/10.1080/10241220902977653.

[49] A.A. Ebrahimi, R. Ghiasi, and C. Foroutan-Nejad. "Topological characteristics of the Ring Critical Points and the aromaticity of groups IIIA to VIA hetero-benzenes.". *Journal of Molecular Structure: THEOCHEM*, **941**:47–52, 2010. DOI: https://doi.org/10.1016/j.theochem.2009.10.038.

[50] R. Ghiasi and A. Moghimi. "Theoretical study of the interactions between borthiin and fluorinated borthiins with difluorine.". *Phosphorus, Sulfur and Silicon and the Related Elements*, **185**:1964–1971, 2010. DOI: https://doi.org/10.1080/10426500903403107.